

# Implementation of the $SP_3$ equations in a MOOSE-based application

Roberto E. Fairhurst Agosta, Kathryn D. Huff

*University of Illinois at Urbana-Champaign, Dept. of Nuclear, Plasma, and Radiological Engineering  
ref3@illinois.edu*

## 1 ABSTRACT

*The Multi-physics Object-Oriented Simulation Environment is a framework that supports the development of applications for solving nonlinear systems of differential equations. This work presents the implementation of an application in that framework for solving the Simplified  $P_3$  equations. We conducted two exercises with results as low as 12 pcm and as high as 145 pcm from the reference results, successfully validating the proposed application.*

## 2 INTRODUCTION

This work presents the implementation of the Simplified  $P_3$  ( $SP_3$ ) equations [1] in a Multi-physics Object-Oriented Simulation Environment (MOOSE)-based application. MOOSE [2] is a computational framework that supports engineering analysis applications. In a nuclear reactor, several partial differential equations describe its physical behavior. These equations are typically nonlinear, and they are often coupled to each other. MOOSE supports the development of applications for solving such systems.

MOOSE is an open-source Finite Element Method (FEM) framework. The framework itself relies on LibMesh [3] and Petsc [4] for solving nonlinear equations. MOOSE-based applications define weak forms of the governing equations and modularize the physics expressions into "kernels." Kernels are C++ classes containing methods for computing the residual and Jacobian contributions of individual pieces of the governing equations. MOOSE and LibMesh translate them into residual and Jacobian functions. These functions become inputs into Petsc solution routines.

All the software built on the MOOSE framework shares the same Application Programming Interface (API), facilitating relatively easy coupling between different phenomena. While the  $SP_3$  equations solve the neutronics in a nuclear reactor, other applications may solve the thermal-fluids, and given they share the same API; their integration is straightforward. Additionally, the framework and its applications use Message Passing Interface (MPI) for parallel communication allowing for deployment on massively-parallel cluster-computing platforms.

The  $P_N$  method [5] discretizes the transport equation by expanding the angular dependence of the neutron flux in spherical harmonics, considering up to order  $N$  polynomials. If  $N \rightarrow \infty$ , the solution of the  $P_N$  equations tends to the exact transport solution. In three-dimensional geometries, the number of  $P_N$  equations is proportional to  $(N + 1)^2$ , whereas, in one-dimensional planar geometries, the number of  $P_N$  equations is  $(N + 1)$ . Gelbard [1] proposed the  $SP_N$  approximation by replacing the second derivatives in the one-dimensional planar  $P_N$  equations with three-dimensional Laplacian oper-

ators. This approximation considerably reduces the number of equations conserving a reasonable accuracy. Capilla et al. [6] conducted an extension of the C5 Mixed-Oxide (MOX) fuel Benchmark [7] introduced by Brantley and Larsen [8] comparing the  $P_3$  and  $SP_3$  methods, the difference between results being less than 40 pcm.

The  $SP_N$  approximation has the disadvantage that the solution does not usually converge to the true transport solution as  $N \rightarrow \infty$ . Additionally, the theoretical basis of Gelbard's formulation of  $SP_N$  approximation was weak. For these reasons, the method did not gain widespread use until the 2000s, when thanks to Pomraning [9], Brantley, and Larsen's [8] contribution, the method gained a stronger theoretical basis.

In practice, the  $SP_N$  equations are most accurate for diffusive problems or for problems in which the solution behaves nearly one-dimensionally and has weak tangential derivatives at material interfaces. For problems with strong, multidimensional transport effects, such as voids, streaming regions, or geometrically complex regions, the  $SP_N$  solutions are less accurate [10]. However, several results show that the  $SP_N$  approximation yields more accurate solutions than the diffusion approximation [11] [12] [13] [14] [15] with considerably less computational expense than the discrete ordinates ( $S_N$ ) method [8]. For example, the  $SP_3$  approximation is preferable over the diffusion approximation for modeling reactors using MOX/ $UO_2$  fuel assemblies. MOX fuel assemblies have higher thermal absorption and fission cross-sections than  $UO_2$  fuel assemblies, and consequently, their thermal flux is lower while their power production higher. Modeling these characteristics using the diffusion approximation may be challenging [8] [6].

The  $SP_3$  approximation gained popularity throughout the last couple of decades and currently, different software uses it to solve the neutron transport equation. Some of those software are SCOPE2 [16], PARCS [10], DYN3D [12], SIMULATE-5 [17], and COCAGNE [13].

## 3 METHODOLOGY

This section describes the methodology followed for solving the equations. Davidson [5] defined the one-dimensional multi-group  $P_N$  equations. For  $N = 3$  and steady-state, the equations become

$$\frac{d}{dx}\phi_{1,g} + \Sigma_{t,g}\phi_{0,g} = \sum_{g'=1}^G \Sigma_{s0,g' \rightarrow g}\phi_{0,g'} + \frac{\chi_g}{k_{eff}} \sum_{g'=1}^G \nu \Sigma_{f,g'}\phi_{0,g'} + Q_{0,g} \quad (1)$$

$$\frac{1}{3} \frac{d}{dx}\phi_{0,g} + \frac{2}{3} \frac{d}{dx}\phi_{2,g} + \Sigma_{t,g}\phi_{1,g} = \sum_{g'=1}^G \Sigma_{s1,g' \rightarrow g}\phi_{1,g'} + Q_{1,g} \quad (2)$$

$$\frac{2}{5} \frac{d}{dx}\phi_{1,g} + \frac{3}{5} \frac{d}{dx}\phi_{3,g} + \Sigma_{t,g}\phi_{2,g} = \sum_{g'=1}^G \Sigma_{s2,g' \rightarrow g}\phi_{2,g'} + Q_{2,g} \quad (3)$$

$$\frac{3}{7} \frac{d}{dx}\phi_{2,g} + \Sigma_{t,g}\phi_{3,g} = \sum_{g'=1}^G \Sigma_{s3,g' \rightarrow g}\phi_{3,g'} + Q_{3,g} \quad (4)$$

where

$\phi_{n,g}$  =  $n^{th}$  moment of group  $g$  neutron flux

$\Sigma_{t,g}$  = group  $g$  macroscopic total cross-section

$\Sigma_{sn,g' \rightarrow g}$  =  $n^{th}$  moment of the group  $g'$  to group  $g$

macroscopic scattering cross-section

$\nu \Sigma_{f,g}$  = group  $g$  macroscopic production cross-section

$\chi_g$  = group  $g$  fission spectrum

$k_{eff}$  = multiplication factor

$Q_{n,g}$  =  $n^{th}$  moment of group  $g$  external neutron source

$G$  = number of energy groups.

Assuming an isotropic external source and a negligible anisotropic group-to-group scattering [8]

$$Q_{n,g} = 0, \quad n > 0$$

$$\Sigma_{sn,g' \rightarrow g} = 0, \quad g' \neq g, \quad n > 0$$

simplifies equations 2 and 4, allowing to express the odd moments of the flux  $\phi_{1,g}$  and  $\phi_{3,g}$  as functions of the even moments  $\phi_{0,g}$  and  $\phi_{2,g}$ . Introducing  $\phi_{1,g}$  and  $\phi_{3,g}$  into equations 1 and 3 reduces the system from four to two equations. Introducing the variables  $\Phi_{0,g}$  and  $\Phi_{2,g}$ , reorganizing the equations, and replacing the second derivatives by Laplacian operators [1] yields the SP<sub>3</sub> equations [12]

$$-D_{0,g}\Delta\Phi_{0,g} + \Sigma_{0,g}\Phi_{0,g} - 2\Sigma_{0,g}\Phi_{2,g} = S_{0,g} \quad (5)$$

$$-D_{2,g}\Delta\Phi_{2,g} + \left(\Sigma_{2,g} + \frac{4}{5}\Sigma_{0,g}\right)\Phi_{2,g} - \frac{2}{5}\Sigma_{0,g}\Phi_{0,g} = -\frac{2}{5}S_{0,g} \quad (6)$$

where

$$\Sigma_{n,g} = \Sigma_{t,g} - \Sigma_{sn,g' \rightarrow g}$$

$$\Phi_{0,g} = \phi_{0,g} + 2\phi_{2,g}$$

$$\Phi_{2,g} = \phi_{2,g}$$

$$D_{0,g} = \frac{1}{3\Sigma_{1,g}}$$

$$D_{2,g} = \frac{9}{35\Sigma_{3,g}}$$

$$S_{0,g} = \sum_{g' \neq g}^G \Sigma_{s0,g' \rightarrow g} (\Phi_{0,g'} - 2\Phi_{2,g'})$$

$$+ \frac{\chi_g}{k_{eff}} \sum_{g'=1}^G \nu \Sigma_{f,g'} (\Phi_{0,g'} - 2\Phi_{2,g'}) + Q_{0,g}.$$

The Marshak-like vacuum boundary conditions (BCs) complete the system of equations [12]

$$\frac{1}{4}\Phi_{0,g} \pm \frac{1}{2}\hat{n} \cdot J_{0,g} - \frac{3}{16}\Phi_{2,g} = 0 \quad (8)$$

$$-\frac{3}{80}\Phi_{0,g} \pm \frac{1}{2}\hat{n} \cdot J_{2,g} + \frac{21}{80}\Phi_{2,g} = 0 \quad (9)$$

where

$$J_{n,g} = -D_{n,g}\nabla\Phi_{n,g}.$$

Finally, multiplying equations 5 and 6 by a test function and integrating over the domain yields the weak form of the equations modularized into kernels in the MOOSE-based application. For brevity, we will not display the derivation of the kernels here. Such procedure is standard in weighted residual methods and can be found in [14] and any finite elements book [18].

## 4 RESULTS

This section presents several numerical results that validate the calculation scheme. Section 4.1 displays the results of a one group exercise presented in [8]. Section 4.2 shows the results of the C5 MOX Benchmark [7].

### 4.1 One group two-dimensional problem

This section describes a one group, isotropic-scattering eigenvalue problem introduced by Brantley and Larsen [8]. This section also presents the result obtained with the SP<sub>3</sub> solver and compares it against the reference value. Figure 1 shows the problem's geometry, and Table I specifies its cross-sections.

We created the mesh using the software Gmsh [19]. The mesh had  $6 \times 10^3$  elements. The simulation convergence criterion was  $10^{-8}$  for the neutron flux.

Table II compares the eigenvalue obtained with the SP<sub>3</sub> solver and the reference value [8] using the equation

$$\Delta\rho = \left| \frac{k_{SP_3} - k_{Ref}}{k_{SP_3} k_{Ref}} \right| \quad (10)$$

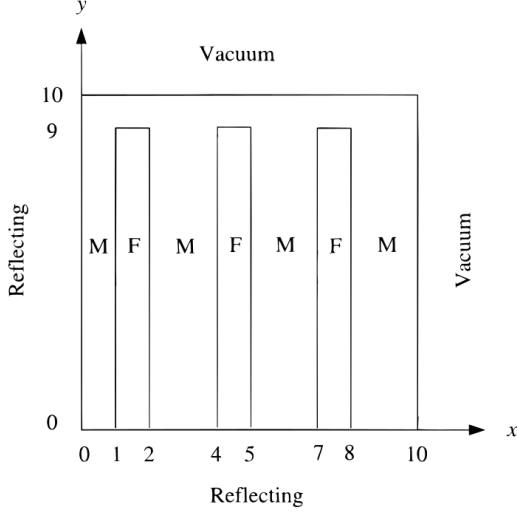


Fig. 1: Geometry of the one group eigenvalue problem. Image reproduced from [8].

Material	$\Sigma_t$	$\Sigma_{s0}$	$\nu\Sigma_f$
M	1.00	0.93	0.00
F	1.50	1.35	0.24

TABLE I: Cross-sections of the one group eigenvalue problem [8]. Values expressed in  $cm^{-1}$ .

where

$$\begin{aligned} \Delta_p &= \text{reactivity difference [pcm]} \\ k_{SP_3} &= \text{eigenvalue obtained with } SP_3 \text{ solver} \\ k_{Ref} &= \text{reference eigenvalue.} \end{aligned}$$

$k_{Ref}$	$k_{SP_3}$	$\Delta_p$
0.79862	0.79854	12

TABLE II: Comparison between the result obtained with the  $SP_3$  solver and the reference result for the one group eigenvalue problem.

## 4.2 C5 MOX Benchmark

This section introduces the C5 MOX Benchmark [7] and presents the  $SP_3$  solver results. The Organisation for Economic Co-operation and Development (OECD)/Nuclear Energy Agency (NEA) developed this benchmark to validate methods and identify their strengths, limitations, and accuracy, and suggest needs for method development. Two types of fuel assembly (MOX and  $UO_2$ ) and a reflector comprise the core, shown in Figure 2. Each fuel assembly consists of a  $17 \times 17$  array of squared pin cells, as displayed in Figures 3 and 4. The dimensions of each pin cell are  $1.26 \times 1.26$  cm, being  $21.42 \times 21.42$  cm the dimensions of each assembly, and 128.52 cm

of the whole core. The benchmark [7] specifies the cross-sections, which have a two-energy group structure.

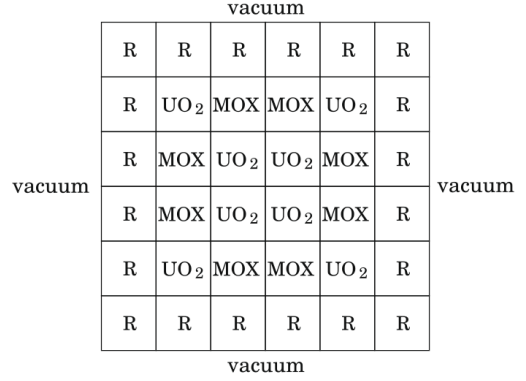


Fig. 2: C5 MOX benchmark configuration.  $R$  corresponds to the reflector region. Image reproduced from [6].

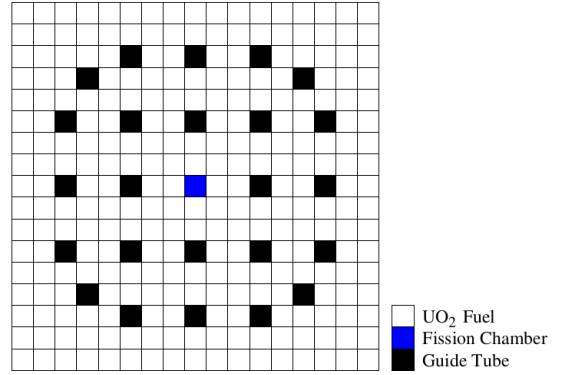


Fig. 3: Structure of the  $UO_2$  assembly. Image reproduced from [6].

When no anisotropic component of the scattering cross-section is available, the benchmark recommends applying the diagonal transport correction

$$\begin{aligned} D_{0,g} &= \frac{1}{3\Sigma_{tr,g}} \\ \Sigma_{tr} &= \Sigma_{t,g} - \bar{\mu}_g \Sigma_{s0,g} \end{aligned} \quad (11)$$

where

$$\begin{aligned} \Sigma_{tr,g} &= \text{group } g \text{ transport cross-section} \\ \bar{\mu}_g &= \text{group } g \text{ average cosine deviation angle.} \end{aligned}$$

For the sake of comparison, we conducted the exercise using the normal scheme and using the transport correction for calculating  $D_{0,g}$  with equations 7 and 11, respectively. Due to the problem's symmetry, the model included only a quarter of the core. The mesh had  $2.4 \times 10^4$  elements. The simulation convergence criterion was  $10^{-8}$  for the neutron flux.

Table III compares the eigenvalues obtained with the  $SP_3$  solver and the references. For the normal scheme, we use

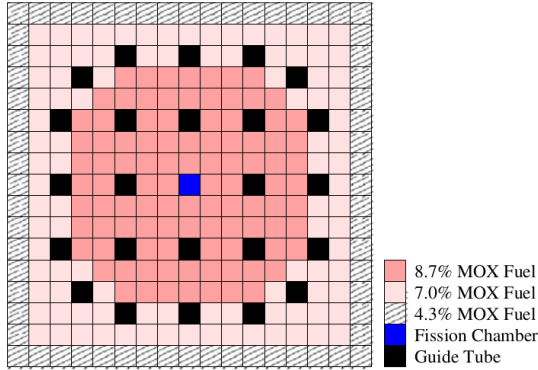


Fig. 4: Structure of the MOX assembly. Image reproduced from [6].

a reference value from Capilla et al. [6]. For the transport correction, we use the reference value from the benchmark [7].

	$k_{Ref}$	$k_{SP_3}$	$\Delta\rho$
Normal scheme	0.96969	0.97106	145
Transport correction	0.93755	0.93792	43

TABLE III: Comparison between the results obtained with the  $SP_3$  solver using the normal scheme (equation 7) and the transport correction (equation 11) and the reference results for the C5 MOX Benchmark.

The results obtained with the  $SP_3$  solver are within the 145 pcm to the reference values. However, the difference between the reference values of the different schemes is 3535 pcm, suggesting that the use of the transport correction is necessary.

Figure 5 presents the power distribution and the relative difference to the reference provided by the benchmark [7]. For brevity, we only calculated the power distribution using the transport correction. The benchmark specifies the power distribution pin-by-pin, but to simplify displaying the results, Figure 5 presents the power distribution in each assembly. The results of the power distribution are within the 1% difference.

## 5 CONCLUSIONS

MOOSE is a computational framework that solves systems of nonlinear differential equations. As part of this work, we implemented the kernels to solve the steady-state  $SP_3$  equations in a MOOSE-based application. Additionally, we carried out two exercises whose reference results were known. The first exercise solved a one-group eigenvalue problem with a simple geometry, with a result within the 12 pcm. The second exercise studied the C5 MOX Benchmark, solving it using different approaches and obtaining results within the 145 pcm. The calculated power distribution values were within the 1% error from the reference.

While the  $SP_3$  equations solve the neutronics in a nuclear reactor, future work may develop other applications to solve the thermal-fluids or integrate this application to existing ap-

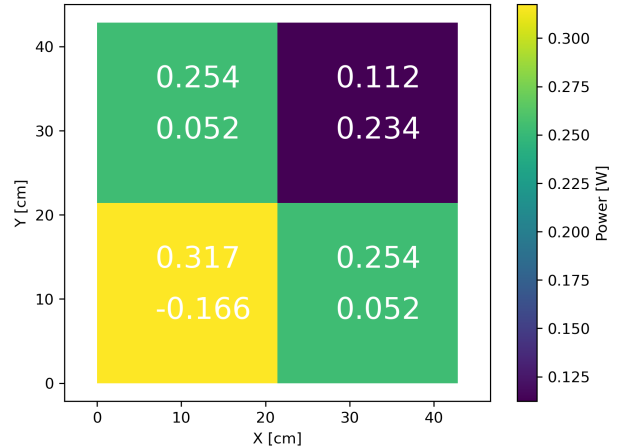


Fig. 5: Power distribution in the C5 MOX Benchmark. Top: power distribution. Bottom: relative difference to reference values expressed in %.

plications. MOOSE-based applications share the same API making their integration straightforward.

## 6 ACKNOWLEDGEMENTS

Roberto E. Fairhurst Agosta and Prof. Huff are supported by the Nuclear Regulatory Commission (NRC) Faculty Development Program (award NRC-HQ-84-14-G-0054 Program B). Prof. Huff is also supported by the Blue Waters sustained-petascale computing project supported by the National Science Foundation (awards OCI-0725070 and ACI-1238993) and the state of Illinois, the DOE ARPA-E MEITNER Program (award DE-AR0000983), the DOE H2@Scale Program (award), and the International Institute for Carbon Neutral Energy Research (WPI-I2CNER), sponsored by the Japanese Ministry of Education, Culture, Sports, Science and Technology.

## REFERENCES

1. E. GELBARD, “Application of spherical harmonics methods to reactor problems,” Technical Report WAPD-BT-20, Bettis Atomic Power Laboratory (1960).
2. D. GASTON, C. NEWMAN, G. HANSEN, and D. LEBRUN-GRANDIÉ, “MOOSE: A parallel computational framework for coupled systems of nonlinear equations,” *Nuclear Engineering and Design*, **239**, 10, 1768–1778 (Oct. 2009).
3. B. S. KIRK, J. W. PETERSON, R. H. STOGNER, and G. F. CAREY, “libMesh : a C++ library for parallel adaptive mesh refinement/coarsening simulations,” *Engineering with Computers*, **22**, 3-4, 237–254 (Dec. 2006).
4. BALAY, BRUNE, BUSCHELMAN, GROPP, KARPEYEV, KNEPLEY, C. MCINNES, RUPP, SMITH, and ZHANG, “PETSc Users Manual,” Tech. Rep. ANL-95/11 Rev 3.14, Argonne National Laboratory (ANL), Lemont, IL (Apr. 2016).
5. B. DAVIDSON, *Neutron Transport Theory*, Oxford University Press, London (1957).
6. M. CAPILLA, D. GINESTAR, and G. VERDÚ, “Applica-

- tions of the multidimensional equations to complex fuel assembly problems,” *Annals of Nuclear Energy*, **36**, 10, 1624–1634 (Oct. 2009).
7. C. CAVAREC, J. PERRON, D. VERWAERDE, and J. WEST, “Benchmark Calculations of Power Distributions within Assemblies,” Technical Report HT-12/94006 A, NEA/NSC/DOC (94) 28, Nuclear Energy Agency Committee on Reactor Physics (1994).
  8. P. BRANTLEY and E. LARSEN, “The Simplified P3 Approximation,” *Nuclear Science and Engineering* (2000).
  9. G. POMRANING, “Asymptotic and variational derivations of the simplified PN equations,” *Annals of Nuclear Energy*, **20**, 9, 623–637 (Sep. 1993).
  10. T. DOWNAR, D. LEE, Y. XU, and T. KOZLOWSKI, “PARCS v2.6 US NRC Core Neutronics Simulator THEORY MANUAL,” Tech. rep., School of Nuclear Engineering Purdue University, W. Lafayette, Indiana (Jun. 2004).
  11. A. MUI, Y. KIM, and D. HARRIS, “Modified P3 transport improvements for reactor diffusion calculations,” Transactions of the American Nuclear Society, Los Angeles, CA, USA (Nov. 1987), vol. 55, pp. 584–586.
  12. C. BECKERT and U. GRUNDMANN, “Development and verification of a nodal approach for solving the multigroup SP3 equations,” *Annals of Nuclear Energy* (2007).
  13. M. FLISCOUNAKIS, E. GIRARDI, T. COURAU, and D. COUYRAS, “Potential of pin-by-pin SPN calculations as an industrial reference,” Chicago, USA (Jun. 2012).
  14. E. H. RYU and H. G. JOO, “Finite element method solution of the simplified P3 equations for general geometry applications,” *Annals of Nuclear Energy*, **56**, 194–207 (Jun. 2013).
  15. M. KHOSRAVI MIRZAEI, A. ZOLFAGHARI, and A. MINUCHEHR, “Reactor core analysis through the SP3-ACMFD approach. Part I: Static solution,” *Nuclear Engineering and Technology*, **52**, 2, 223–229 (Jul. 2019).
  16. M. TATSUMI and A. YAMAMOTO, “Object-Oriented Three-Dimensional Fine-Mesh Transport Calculation on Parallel/Distributed Environments for Advanced Reactor Core Analyses,” *Nuclear Science and Engineering* (Jul. 2002).
  17. T. BAHADIR and S.-O. LINDAHL, “Studsвик’s Next-Generation Nodal Code, SIMULATE-5,” American Nuclear Society, South Carolina, USA (Apr. 2009), p. 12.
  18. A. QUARTERONI and A. VALLI, *Numerical Approximation of Partial Differential Equations*, no. 23 in Springer Series in Computational Mathematics, Springer-Verlag, Berlin, Heidelberg (1994).
  19. C. GEUZAIN and J.-F. REMACLE, “Gmsh: a three-dimensional finite element mesh generator with built-in pre- and post-processing facilities,” *International Journal for Numerical Methods in Engineering* (2009).